© January 2020 | IJIRT | Volume 6 Issue 8 | ISSN: 2349-6002

Multi-Atlas Image Segmentation of Thoracic & Abdominal Anatomy

Pooja Waghmare[1], M. D. Mali[2], and S. P. Sagat[3]
[1]*PG Student, N. B. N. Sinhgad Institute College of Engineering, Solapur*
[2,3]*Assistant Professor, N. B. N. Sinhgad Institute College of Engineering, Solapur*

***Abstract*- Image segmentation is a concept that describes removal of or extraction of part of the image that contains meaningful data in comparison with the whole image. The main objective of segmentation is region partitioning that are different on visual basis or property wise and/or characteristically meaningful. Accurate segmentation of human anatomy is critically fundamental as well as most time consuming task in medical planning. This is required mainly for medical diagnosis, qualitative analysis & treatment planning. Atlas based segmentation approach guides the segmentation process relying on the concept of an atlas & the target subject image. Atlas is nothing but an already pre-segmented reference image volume validated by an expert that includes structure of interests. The atlases are mapped with the image to be segmented.**

***Index terms*- Atlas segmentation; image registration; level sets, Multi Atlas Fusion.**

I.INTRODUCTION

The main goal of this technique is to develop new methodologies that can potentially improve the accuracy and reliability of atlas-based segmentation. It is evident from the discussions presented in the preceding sections that there are mainly two important components that have a significant impact on the quality of automated segmentations: first, the non-rigid registration approach used for finding out the point-by-point mapping between the atlas and the target images; second, the fusion strategy used for merging segmentation results obtained from multiple atlases. The main objective of this project is to design a new atlas segmentation system for thoracic & abdominal anatomy. The objective will be fulfilled from the proposed system are as follows:

1) Usage of a multi-atlas approach to better identify organ shapes & locations

2) Usage of a multi-modality algorithm capable of coping with variability in contrast & Hounsfield Unit calibration.

3) To refine the segmentation boundaries obtained in the multi-atlas segmentation.

The main objective of segmentation is region partitioning that are different on visual basis or property wise and/or characteristically meaningful. Accurate segmentation of human anatomy is critically fundamental as well as most time consuming task in medical planning. This is required mainly for medical diagnosis, qualitative analysis & treatment planning.

II. WORK FLOW OF THE AUTOMATED ATLAS-SEGMENTATION APPROACH

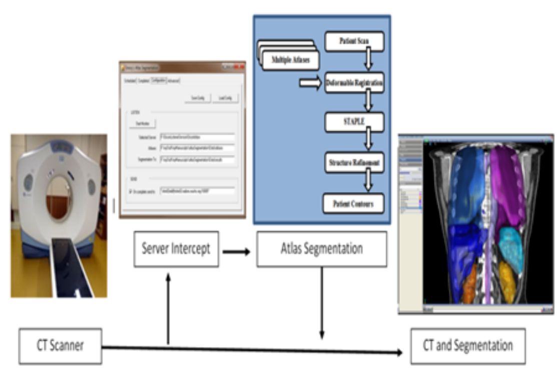

Fig.1. Work flow of the automated atlas-segmentation approach

A. Dataset

Datasets used for validation are all clinical scans acquired on the institution's scanner (Light Speed RT 16; GE Medical Systems, Waukesha, WI) using the standard acquisition protocol for abdomen and thorax in a two-month period while developing the proposed approach. All datasets were used for the validation, independent of patient size, acquisition protocol, patient positioning or treatment site. On our scanner, both abdominal and thoracic scanning protocols produce images of 2.5 mm voxel size, with a typical scan having 100 to 200 slices depending on the field of view size that was 40 cm for the abdominal and 50 cm for the thoracic scans.

B. Image registrations

Image registrations were applied on organ-specific cropped images using a leave-one-out scheme among the 20 testing subjects. The organ-specific ROIs were defined by padding 5 cm to each side of bounding boxes to include adequate background tissues. The bounding boxes were estimated using RF for the target, while derived from the manual segmentations for the atlases. Affine followed by non-rigid registrations using NiftyReg [18] were performed to align the atlases to the target; both stages involved five coarse-to-fine levels, and limited the upper intensity threshold to 500.

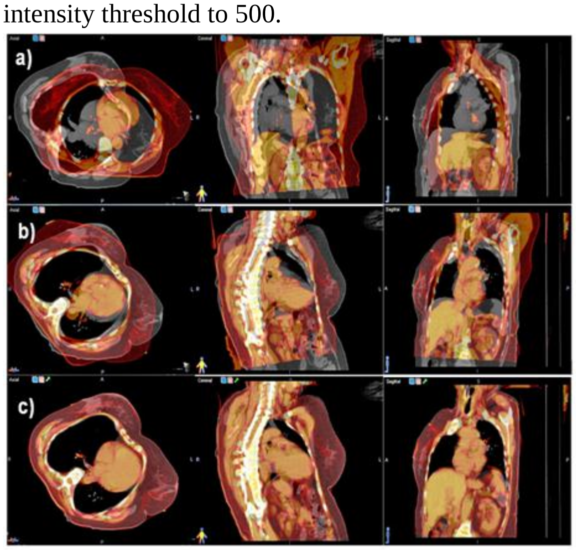

Fig. 2. Steps of the atlas matching procedure show in axial, coronal, and sagittal planes, one atlas dataset

C. Multi Atlas Fusion

Organ-specific atlas selection was performed based on the re-formulated SIMPLE [42, 127] algorithm from the perspective of EM. Consider a collection of R registered atlases with label decisions, $\boldsymbol{D} \in \boldsymbol{L}N{\times}R$, where N is the number of voxels in each registered atlas, and $\boldsymbol{L} = \{0,1, \dots, L-1\}$ represents the label sets. Let $\boldsymbol{c} \in \boldsymbol{S}R$, where $\boldsymbol{S} = \{0,1\}$ indicates the atlas selection decision, i.e., 0 – ignored, and 1 – selected. Let i be the index of voxels, and j of registered atlases. A non-linear rater model, $\theta \in \mathbb{R}R{\times}2{\times}L{\times}L$, considers the two atlas selection decisions.

Let the ignored atlases be no better than random chance, and the selected atlases be slightly inaccurate with error factors $\boldsymbol{\epsilon} \in \mathbf{E}\mathrm{R}{\times}1$, where $\mathbf{E} \in (0, L{-}1)$. Thus

$1\ 1 - \epsilon j,\ s' = s$

$\theta j0s's =, \forall s'\ ;\ \theta j1s's\ = \{\ \ \epsilon j\ '$

$L\ L\ -1\ ,\ s \neq s$

III. MULTI-ATLAS FUSION SEGMENTATION

Multi-atlas fusion segmentation is applied for the nine different CT scan images from patient's database. The following figure shows

Fig. 3. Input image

Segmentation of large organ tissue liver , soft tissue organ stomach and low contrast tissue aorta have been performed step by step and / or in a one run go. Following figure 4 shows the complete segmentation of liver, stomach and aorta region from the given "Input image" shows in figure 3.

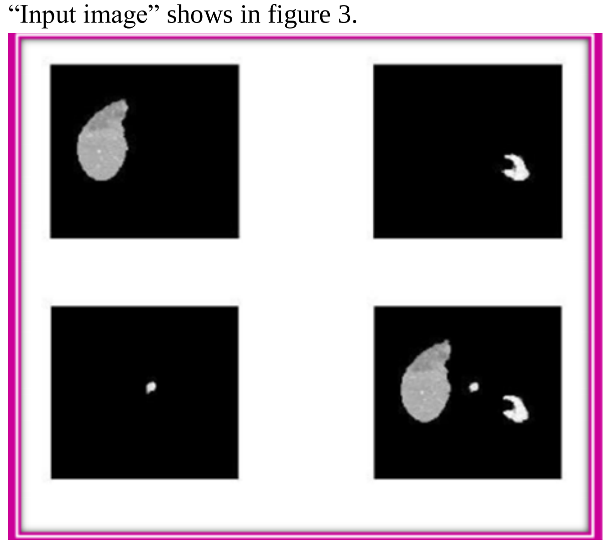

Fig 4. Complete segmented

Many different features are extracted from the different set of patient's original CT scan images. These features are namely contrast, correlation, homogeneity, entropy, mean, standard deviation, entropy, root mean square values, variance, smoothness, kurtosis & skewness values. These extracted features for figure.3 are tabulated in the following tabular form.

1	2	3	4	5	6	7	8	9
Images	Contrast	Correlation	Energy	Homogeneity	Mean	Standard Deviation	Entropy	RMS
OImg	0.17106	0.981	0.23469	0.92637	68.0375	74.8773	5.3998	11.4974
Seg1	0.093413	0.975	0.82873	0.98972	15.2302	48.5327	1.0867	2.5467
Seg2	0.055055	0.950	0.97338	0.99715	2.933	25.8263	0.24649	0.75107
Seg3	0.021109	0.887	0.99465	0.99895	0.52734	10.6275	0.063022	0.20467
Final seg	0.16958	0.965	0.79982	0.98583	18.6906	55.017	1.3522	3.5024

Table .1 Overall segmentation properties

In the above table 1, notations given of seg1, seg2, seg3 and final seg are denoted for liver segmentation, stomach and aorta segmentation images respectively. From the achieved algorithm it has been shown that the extracted parameters through overall segmentation process are in the standard specified range [9].

In our approach with the help of mesh and 3-D contour plots of segmented image along with the original image, it is possible to detect the exact location, shape and size of organs though the irregularities, overlapping of organs were present in the original images.

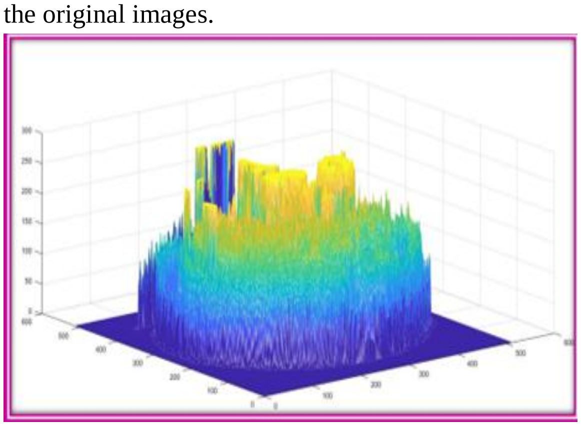

Fig. 5 Mesh contour plot of original image

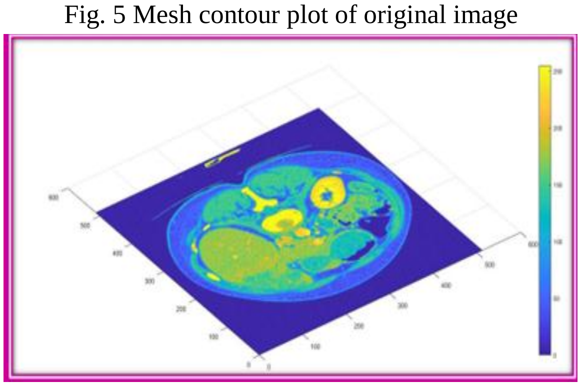

Fig. 6 Mesh contour-2 plot of original image

Following fig. 7 & 8 shows mesh contour plots for overall segmented image.

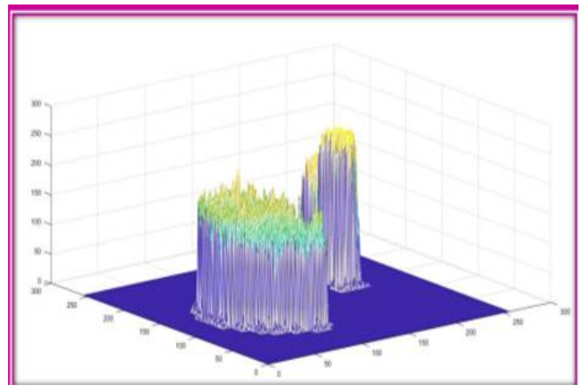

Fig. 7 Mesh contour plot of overall segmented image

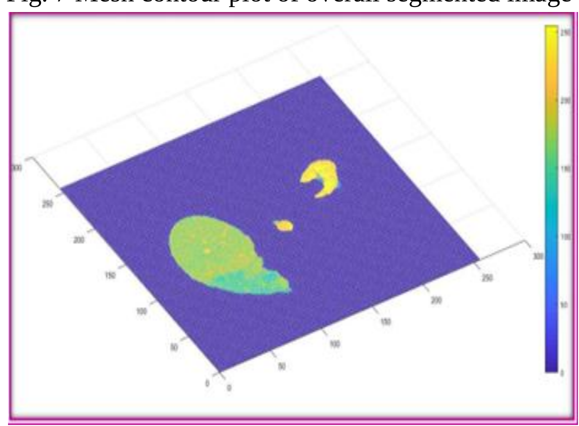

Fig. 8 Mesh contour-2 plot of overall segmented image

Minimal execution time (sec) is achieved through our proposed work. Given table .2 Shows processing time in seconds for different original images which includes execution time for segmentation of liver, stomach, aorta and overall segmentation of these

ORGAN	IMAGE 1	IMAGE 2	IMAGE 3	IMAGE 4	IMAGE 5	IMAGE 6	IMAGE 7
LIVER	6.76487	6.4663	9.5333	6.7032	7.1483	6.4733	29.5843
STOMACH	12.1186	11.8853	13.6748	11.8327	12.159	12.0197	37.204
AORTA	17.2731	17.2447	19.6011	17.3025	17.2488	17.4329	43.8415
Over All Segmentation	37.574	36.7572	44.1619	37.6638	37.6999	37.0747	115.998

three organs in one go. From above table, it's clearly indicated that the performance time ranges from 6.5 sec to maximum 9.5 sec for liver segmentation , from 11.9 sec to 14 sec for stomach and 17 sec to 21 sec for aorta. In the worst case the max time recorded for the segmentations are 29.5 sec for liver , 37.2 sec for stomach and 43.84 sec for aorta. The overall time required for segmentation of all organs in the above cases is varying within the range of 36.75 sec to 44.16 sec. In the worst case for our approach this has been recorded as 115.99 sec. This shows proposed algorithm executes within less time, without compromising with the quality and accuracy of the segmentation [5].

VI.CONCLUSION

This approach will produce an accurate segmentation results even within the context of the variability in image shape & quality encountered in the course of standard image acquisition in the clinic. These methods have the potential to significantly improve the efficiency & accuracy of radiation treatment planning. It has been recorded minimal execution or performance time with better quality segmentation.

REFERENCES

[1] H.Narkhede, "Review of image segmentation techniques," Int. J. sci. Mod. Eng, vol. 1, p 28,2013.
[2] Zhang X, Tian J, Deng K, Wu Y, Li X. Automatic liver segmentation from CT scans based on a statistical shape model. Conf Proc IEEE Eng Med Biol Soc. 2010;2010:5351–54.
[3] Campadelli P, Casiraghi E, Pratissoli S. A segmentation framework for abdominal organs from CT scans. Artif Intell Med. 2010;50(1):3–11.
[4] H.Zhuang, K.-S. Low, and W-Y. Yau, Multichannel pulse-coupled-neural-network-based color image segmentation for object detection," IEEE Transactions on Industrial Electronics. vol. 59, pp. 3299-3308,2012.
[5] Eduard Schreibmann, a David M. Macrus, Tim Fox, "Multi-atlas segmentation of thoracic and abdominal anatomy with level-set based local search ", Journal of Applied Clinical Medical Physics, vol. 15, No.4, 2014.
[6] Y. Liu and Y. Yu, "Interactive image segmentation based on level sets of probabilities." IEEE Transactions on Visualization and Computer Graphics, vol. 18, pp. 202-213, 2012.
[7] V. A. Prisacariu and I. Reid, "Nonlinear shape manifolds as shape priors in level set segmentation and tracking," in IEEE Conference on Computer Vision and Pattern Recognition (CVPR). 2011 2011. pp. 2185-2192.
[8] H. Yu, E. S. Barriga, C. Agurto, S. Echegaray, M. S. Pattichis, W. Bauman, et al., " Fast localization and segmentation of optic disk in retinal images using directional matched filtering and level sets," IEEE Transactions on Information Technology in Biomedicine, vol. 16, pp. 644-657, 2012.
[9] M. W. Law and A. Chung. " Segmentation of intracranial vessels and aneurysms in phase contrast magnetic resonance angiography using multi-range filters and local variances," IEEE Transactions on Image Processing, vol. 22, pp. 845-859,2013.
[10] Ramus L, Commowick O, Malandain G. Construction of patient specifc atlases from locally most similar anatomical pieces. Med Image Comput Comput Assist Interv. 2010;13(pt 3):155–62.
[11] L. Sorensen, M. Nielsen, P. Lo, H. Ashraf, J. H. Pedersen, and M. De Bruijne, "Texturebased analysis of COPD: a data-driven approach," IEEE Transactions on Medical Imaging, vol. 31, pp. 70-78, 2012.
[12] Koti agyeman, CUNY city college, "Automatic Optimum Atlas selection for Multi-Atlas Image Segmentation using Joint Label fusion" City University of New York (CUNY), Cuny Academic Works, 2017.